BBAA VI International Colloquium on:
Bluff Bodies Aerodynamics & Applications
Milano, Italy, July, 20-24 2008

INSTANTANEOUS PRESSURE DISTRIBUTION ON SQUARE CYLINDER IN TURBULENT FLOW

Sungsu Lee[*] and Chan Wook Park[†]

[*] School of Civil Engineering
Chungbuk National University, Cheongju, 361-763, Chungbuk, South Korea
e-mail: joshua@cbnu.ac.kr

[†] Division of Integrated Technology
Daebul University, Gollanamdo, Korea
e-mails: cwpark@mail.daebul.ac.kr

Keywords: Large Eddy Simulation, Instantaneous Pressure.

Abstract. *In this paper, the instantaneous pressure distribution on a square cylinder at the Reynolds number of 22,000 is simulated using the large eddy simulation with the Smagorinsky model for parametrization of the subgrid scales. The finite element formulation is employed for spatial discretization and unsteady computations incorporating a subcycling strategy are performed using the explicit method with streamline upwind scheme for the advection. No-slip condition is enforced on the wall surface. In order to verify present results, simulated three-dimensional wake structures are compared with numerical and experimental results reported by other researchers, which show that dynamics of the vortex-shedding phenomenon are numerically well reproduced using the present method of finite element implementation of large eddy simulation. The simulated pressure distribution on the square cylinder shows that the reattachment was shown to be responsible for the increase in local pressure and random and intermittent processes of reattachment and detachment of the separated shear layer on the cylinder surface were identified.*

1 INTRODUCTION

Dynamic performance of many engineering structures of cylindrical geometry is governed mainly by the interaction between incoming flow and the structure itself. Recent high rise buildings and long-span bridges are especially susceptible to the flow-structure interactions, including aeroelastic effects associated with vortex-induced oscillation, flutter, galloping and buffeting. Hence, of practical interest is subjacent physics of pressure distribution on the surface of the slender bodies. In order to investigate the flow field and pressure distribution around such structures, a study was conducted for numerical computations of unsteady flows around a square cylinder which has sharp corners.

This paper presents a finite element computations of flow field around a 3D square cylinder at Re=22,000. Galerkin finite element method is implemented except for the advection where streamline-upwind scheme is employed. Linear, isoparametric elements are

employed. For the flow at high Reynolds number, the large eddy simulation is employed. Recently, a successful simulation of a turbulent flow around a square cylinder using was reported using the computational method adopted here [1, 2]. In the formulation of large eddy simulation, the Smagorinsky subgrid scale model is employed. The coefficient of eddy viscosity is computed at each time step. Time integration is accomplished using an explicit time integration scheme with subcycling strategy. Pressure is solved for using a segregated Poisson equation at each time step. Uniform flow is employed as inflow, while free slip condition is on lateral boundaries, and no-slip condition is on the solid wall.

2 FORMULATIONS

With box filter applied for space, governing equations consist of Navier-Stokes equations (NSEs) leading to

$$\frac{\partial \overline{u}_i}{\partial t} + \overline{u}_j \frac{\partial \overline{u}_i}{\partial x_j} = -\frac{1}{\rho}\frac{\partial P}{\partial x_i} + \nu \frac{\partial \overline{S}_{ij}}{\partial x_j} - \frac{\partial \hat{\tau}_{ij}}{\partial x_j} \tag{1}$$

where

$$\hat{\tau}_{ij} = \tau^*_{ij} - \tfrac{1}{3}\delta_{ij}\tau^*_{kk\,ij}, \quad P = \overline{p} + \tfrac{1}{3}\tau^*_{kk\,ij} \tag{2}$$

Smagorinsky model based on the eddy viscosity concept and the mixing length theory is employed, where the eddy viscosity concept leads to the following model:

$$\hat{\tau}_{ij} = -2\nu_{SGS}\overline{S}_{ij}\,. \tag{3}$$

where ν_{SGS} is the eddy viscosity for LES which has the form of

$$\nu_{SGS} = \left(C_S\Delta\right)^2\sqrt{2\overline{S}_{ij}\overline{S}_{ij}} \tag{4}$$

where C_S is the Smagorinsky constant set to 0.1 in this study.

Applying GFEM with isoparametric elements to governing equations results in the following algebraic equations.

$$\mathbf{M}\dot{\mathbf{V}} + \mathbf{K(V)V} - \mathbf{CP} = \mathbf{Q} \quad \text{and} \quad \mathbf{C}^{\mathrm{T}}\mathbf{V} = \mathbf{0} \tag{5}$$

where **V** is a global velocity vector, **P** is a global pressure vector, and **Q** is a force vector incorporating the velocity natural boundary conditions. **M** is the mass matrix and **K** contains the advection and the diffusion terms. **C** is the gradient matrix while its transpose, $\mathbf{C}^{\mathbf{T}}$ is the divergence matrix. The Reynolds SGS stress term is included in **K** and the eddy viscosity ν_{SGS} is evaluated at the centroid of each element, at each time step. Explicit (Euler) method is employed for time integration, which a Poisson equation is solved for the pressure field at each time step, and the initial flow field is set to zero except for the inflow boundary, and it is next modified to satisfy the continuity equation by solving an auxiliary Poisson equation. Fig (1) depicts the computational domain employed in this study. No-slip on the solid wall and traction free on the outflow boundary are imposed.

3 INTEGRAL PARAMETERS

In order to verify the computational results of the present study, integral parameters are compared with others in Table (1). The computation results in 0.134 as the Strouhal numbers found at the frequency where the peak of the spectral distribution of lift coefficient is located. It is close to the experimental value of 0.13 measured by Lin et al [5, 6]. The drag coefficient is 2.06 and the time-averaged lift coefficient predicted is $O(10^{-2})$. These results are in good

agreement with other experimental and computational data. The time-averaged (mean) streamwise (x-direction) velocity along the line of symmetry is compared in Fig (2) with the experimental data of Lyn et al [5], Durao [6] and other computational results, in which spanwise averaging is carried. The present results are in good agreement with experimental data with a slightly shorter recirculation length.

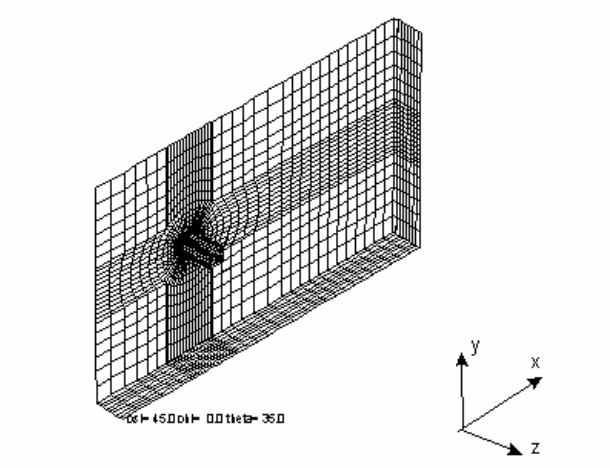

Figure 1. Computational Domain

Table 1. Comparison of integral parameters.

Cases		Re	St	C_D		$(C_L)_{rms}$	l_r
				Mean	rms		
Present	3D LES (SM)	22000	0.134	2.06	0.33	1.214	0.75
Murakami and Mochida[3]	3D LES (SM)	22000	0.132	2.09	-	-	0.64
Lyn et al [4,5]	Experiment	21400	0.132-0.134	2.1	-	-	0.88

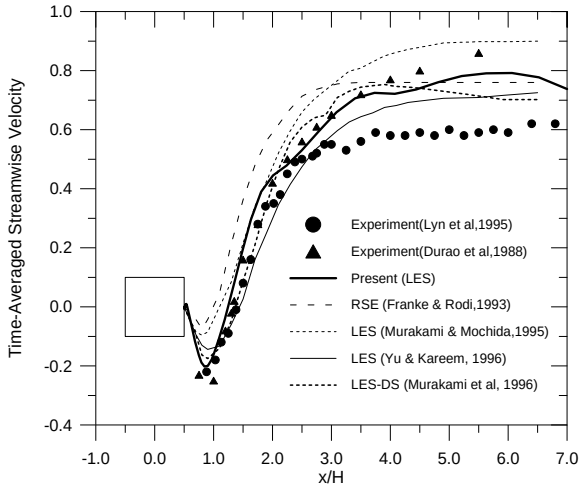

Figure 2. Time-averaged horizontal streamwise velocity along center

4 PRESSURE DISTRIBUTION ON SQUARE CYLINDER

The time-averaged pressure coefficient on the surface of the square cylinder is compared in Fig (3) with the experimental data of Bearman and Obasaju [7] and with the computational results reported by other researchers. On the windward face, the compared data are almost identical to each other, whereas they differ on the side and the leeward faces. The present result shows close agreement with the experimental data, except for the region near the windward corner on the side face. The data are also in good agreement with the results of Murakami *et al* [8] who employed dynamic SGS model, whereas the result of Yu and Kareem [9] shows a large departure on the side wall. The discrepancy between the present results and the reported computational data is attributed to differences in the Reynolds number and the numerical approach employed.

In order to investigate the instantaneous flow field around the square cylinder, five representative instances were defined using lift coefficients. Those instants were referred to a '*Frames*' and depicted in Fig (4). Fig (5) which shows the contour plots of instantaneous pressure coefficients on the surfaces of the square cylinder at the instant corresponding to Frame 5 in Fig (4). Each plot corresponds to a side of the square cylinder as depicted in a small diagram. Apparently the pressure on the lower surface is higher than that on the upper surface, resulting in positive lift (frame 5). Close to the windward corners, concentrations of pressure gradients of large magnitude are observed. Pressure distribution on the windward face is fairly uniform in spanwise direction (z) due to the uniformity of inflow. A mild uniformity of pressure is exhibited on the lower surface where the pressure is higher than that on the upper surface, whereas a large area of low pressure is seen on the upper surface. On the other hand, relatively large changes of pressure distribution in the z-direction are shown on the leeward face due to the three-dimensional characteristics of vortex shedding behind the cylinder.

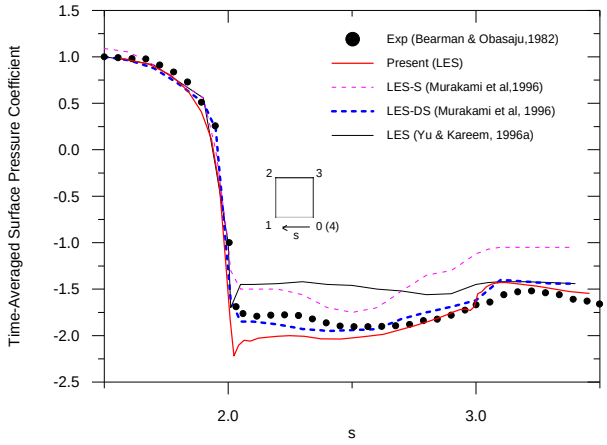

Figure 3. Time averaged pressure distribution on square cylinder

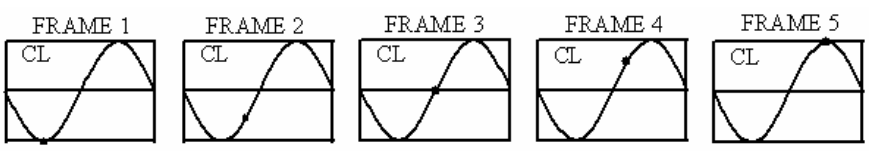

Figure 4: Definition of frames in instantaneous flow field.

It is well recognized that random reattachments of a separated shear layer creates intermittent recirculation regions on the upper and lower walls of the cylinder where lower pressure is expected. In order to investigate this feature, instantaneous flow fields adjacent to the cylinder and pressure distributions on the surface were considered.

A sequence of pressure distributions on the upper wall of the cylinder is shown in Fig (6), each of which corresponds to the frames 1, 3 and 5. The figures also include surface-elevated plots of horizontal velocity and contour plots of lateral velocity adjacent to the surface. In the surface-elevated plots in Fig (6), positive values are flattened out so that the recirculation regions can be visualized.

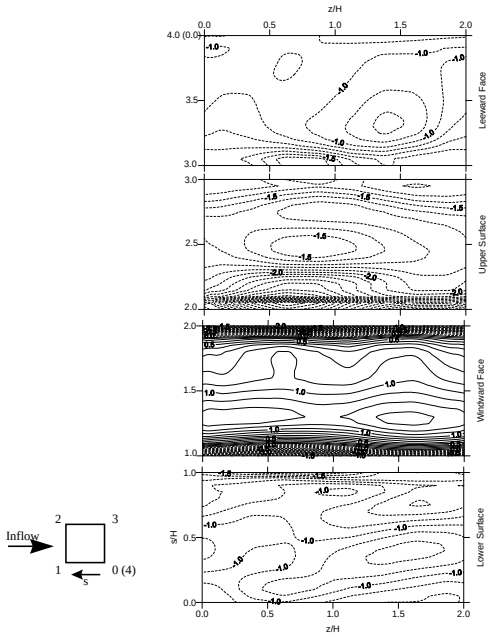

Figure 5. Instantaneous pressure at frame 5

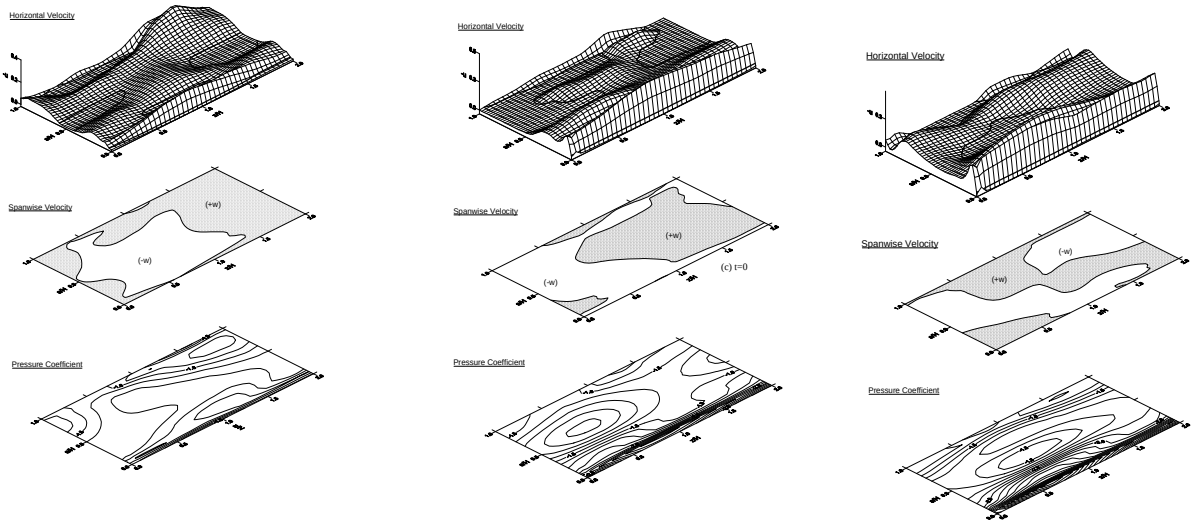

Figure 6. Instantaneous pressure and velocity on upper wall at frames 1, 3 and 5 from left

In the surface-elevated plots of negative horizontal velocity, contours with thick solid line indicate the boundary of the recirculation regions. For all the frames considered here, a large magnitude of negative horizontal velocity is observed close to the windward corners, indicating separation of the incoming flow. The separation is often followed by immediate reattachment resulting in a large gradient of pressure, depending on the spanwise location. Comparing the surface-elevated plots with the pressure contours, the high pressure zone is seen in the region where reattachment occurs. Local detachment of the reattached flow is also observed. The variation of the surface-elevated plots in time and space does not show any particular patterns and confirms that the process of reattachment and detachment is random and intermittent.

The present study does not include a systematic investigation of the influence of aspect ratio on the flow field, but indirect assessment of the quality of the present approach is possible using a spanwise correlation of pressure. In the three-dimensional computation presented here, a periodic condition was imposed on the lateral boundaries normal to the spanwise direction (z), while the length of cylinder is fixed at 2H. In order to compare the present result with the experimental data of Vickery [10], the spanwise correlation was calculated along the center line of the cylinder. In Fig (7), A and B are located at the center line of the upper surface of cylinder, while A' and B' are on the lower surface. The pressure differences between A and A' $\left(\Delta p_A\right)$ and B and B' $\left(\Delta p_B\right)$ were selected as the correlated variables. Denoting the distance between A and B as *r*, a spatial cross-correlation coefficient of pressure is defined as

$$R(r) = \frac{\overline{\Delta p_A \Delta p_B}^{t}}{\sigma_A \sigma_B} \tag{6}$$

where σ_A and σ_B are standard deviations of Δp_A and Δp_B , respectively.

Fig (8) shows the calculated coefficient of spanwise correlation compared with the experimental results of Vickery [10]. One of the implications of the experimental results is that a flow becomes less correlated and vortex shedding is nonuniform and irregular in the spanwise direction when the inflow is turbulent. Due to the periodic condition used, only half of the cylinder length H was considered for the computed case. Since an uniform inflow was imposed in the present computation, the computed values of the correlation coefficient were expected to be close to the experimental data with smooth inflow. The results indicate that the present computation reproduced a slightly less correlated pressure distribution in the spanwise direction, compared to the experimental results. However, the general behavior of the computed coefficient is in reasonable agreement with the experimental data.

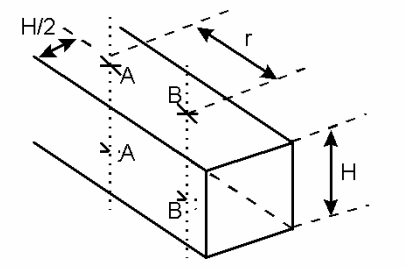

Figure 7. Schematic diagram for spanwise pressure correlation

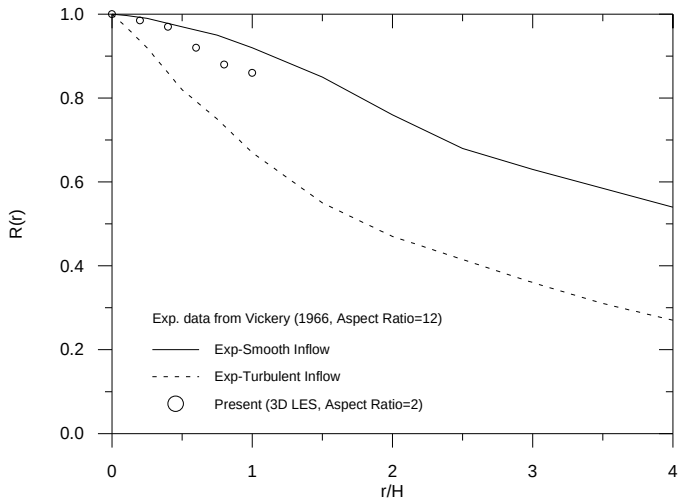

Figure 8. Spanwise Correlation Coefficients of Pressure Difference across Center Line of a Square Cylinder

It was well recognized that turbulence causes intermittent reattachment of the separated shear layer on the upper surface of a cylinder. In addition, an early reattachment (i.e. short recirculation length) increases the curvature of the shear layer, resulting in an increase in the magnitude of negative peak pressure in the region [11]. In order to investigate this feature, negative peak values of pressure on the side wall and the recirculation lengths measured from the windward corners were simultaneously recorded at each time step during the unsteady computation,. Fig (9) depicts the scatter plot of those two variables. A strong dependency between these variables is illustrated: the shorter the recirculation length, the lower the negative peak pressure.

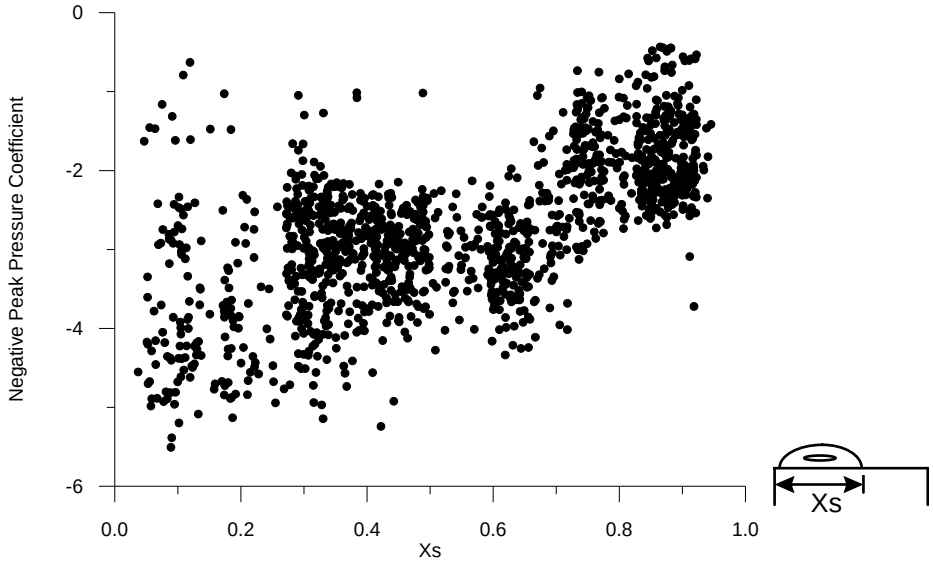

Figure 9. Scatter Plot of Negative Peak Pressure vs. Recirculation Length on Upper Wall of a Square Cylinder

5 CONCLUSION

In order to understand the correlation of surface pressure and flow field, large eddy simulation of 3D turbulent flow around a square cylinder was carried out. The simulated

three-dimensional distributions of the pressure on the surface of the cylinder showed the nonuniformity of the pressure field in the spanwise direction. Random and intermittent processes of reattachment and detachment of the separated shear layer on the cylinder surface were identified, and the reattachment was shown to be responsible for the increase in local pressure. A spanwise correlation of the simulated pressure field was compared to the available experimental data and showed reasonable agreement. In addition, an intermittent reattachment of short recirculation length was shown to be responsible for large negative pressure on the surface.

ACKNOWLEDGEMENTS

This work was supported by the grant from Natural Hazard Mitigation Research Group (Grant No., NEMA-08-NH-02), South Korea

REFERENCES

[1] S. Lee, Large eddy simulation of flow past a square cylinder using finite element method, Ph.D Dissertation, Colorado State University, Ft. Collins, USA, 1997.

[2] S. Lee, Numerical study of wake structure behind a square cylinder at high Reynolds number, *Wind and Structures, Int. J.*, vol.1, no.2, pp.127-144. 1998.

[3] S. Murakami, A. Mochida and K. Hibi, Three-dimensional numerical simulation of air flow around a cubic model by means of large eddy simulation *J. Wind Eng. Ind. Aerodyn., Vol. 25*, 1987, pp.291-305.

[4] D.A. Lyn and W. Rodi,The flapping shear layer formed by flow separation from the forward corner of a square cylinder, *J. Fluid Mech.*, vol. 267, 1994, pp.353-376.

[5] D.A. Lyn, S. Einav, W. Rodi, and J.-H. Park, A laser-Doppler velocimeter study of ensemble-averaged characteristics of the turbulent near wake of a square cylinder, *J. Fluid Mech.*, vol. 304, 1995, pp.285-319.

[6] Durao, D.F.G., M.V. Heitor, and J.C.Pereira (1988), Measurements of turbulent and periodic flows around a square cross-section cylinder, *Exp. Fluids*, vol 6., pp.298-304.

[7] Bearman, P.W., and E.D. Obasaju (1982), An experimental study of pressure fluctuations on fixed and oscillating square-section cylinders, *J. Fluid Mech.*, vol.119, pp.297-321.

[8] Murakami, S., A. Mochida, and S. Iizuka (1996), New trends in turbulence models for prediction of wind effects on structures, *IWEF Workshop on CWE/CFD for Pred. Wind Effects on Structures*, Fort Collins, USA, Aug.

[9] Yu, D.-H., and A. Kareem (1996b), Numerical simulation of flow around rectangular prism, *2nd Int. Conf. Comp. Wind Engr*., Ft. Collins, USA, Aug.

[10] Vickery, B.J. (1966), Fluctuating lift and drag on a long cylinder of square cross-section in a smooth and in a turbulent stream, *J. Fluid Mech.*, vol. 25, part 3, pp.481-494.